Jordanian Journal of Computers and Information Technology (JJCIT), Vol. 10, No. 01, March 2024.

KOCH FRACTAL OCTAGONAL ANTENNA WITH A COMPACT DESIGN AND DEFECTED GROUND STRUCTURE (DGS) FOR ULTRA-WIDEBAND (UWB) WIRELESS USAGE

Tejaswita Kumari, Abu Nasar Ghazali and Anupama Senapati

(Received: 3-Nov.-2023, Revised: 28-Dec.-2023, Accepted: 21-Jan.-2024)

ABSTRACT

This paper introduces a Koch fractal octagonal antenna designed for the ultra wideband (UWB) frequency range. The utilization of the Koch fractal in the antenna design contributes to size reduction and provides compactness in the antenna for UWB. Additionally, it has been noted that the Koch fractal offers wideband operation. The antenna employs copper as the conductor material and Flame Retardant-4 (FR-4) serves as the substrate. The substrate has a dielectric constant ϵr =4.4, a loss tangent tanδ=0.02 and a thickness (h) of 1.6 mm. The overall antenna's dimensions are 34.3 × 26.5 × 1.6 and its electrical dimensions are 0.68λ0 × 0.53λ0 × 0.032λ0. It achieves a maximum gain of 8.94 dBi at a frequency of 12.25 GHz, offering a broad bandwidth ranging from 2 GHz to 12.1 GHz. This antenna exhibits resonance at three distinct frequencies; namely, 3.3 GHz, 6 GHz and 8.6 GHz, making it highly efficient with an overall efficiency of 96.8%. The time-domain characteristic of the antenna is acceptable for UWB, group delay is 1.1 ns, the proposed antenna has a high-fidelity factor of 90.2 and the correlation coefficient is 0.9, which makes the antenna a good candidate for UWB. Due to its performance characteristics, this proposed antenna is wellsuited for short-range wireless personal area networks (WPANs), supporting high-data-rate applications, like Bluetooth and wireless USB and Wireless Body Area Network (WBAN) applications. Its proficiency also extends to industrial settings, where it helps with precision in control systems, asset tracking and short-range sensing and radar systems.

KEYWORDS

Koch fractal geometry, UWB, DGS, Group delay, Correlation coefficient, Fidelity factor, Octagonal, WBAN, WPAN.

1. INTRODUCTION

In the modern era, ultra-wideband antennas encounter many challenges, such as miniaturization, cost-effectiveness, small size, mechanical robustness, attaining high-performance characteristics, like good gain and large bandwidth to accommodate wireless security and wireless data. Due to the need for overcoming these issues, developing a UWB antenna for wireless communication is complex in the operational bandwidth of 3.1-10.6 GHz as per FCC [1]-[2].

The abovestated limitations of UWB antenna, can be resolved by using fractal geometry. Fractal UWB antennas can be leveraged in IoT for data transmission and reception, sensing, location identification and positioning. In UWB antenna design, the main focus is on compactness, miniaturization and wide bandwidth and the design should be direction-independent.

Therefore, the properties of self-similarity and space-filling make fractal geometry a good candidate for UWB antenna design [3], because fractal geometry leads to an enhancement in the antenna's performance. From the previous research done by many researchers [4][5][6], it's known that fractal main sub-classes are mass and boundary. Mass fractal is used for wideband multiband applications. There are so many fractal structures, like Koch, Hilbert, Minkowski, Peano and Sierpinski [4] for reducing the size of the antenna, miniaturization and wideband. Asymmetrical shape and curvature in the geometry of fractals bring the eyes of researchers as well as industries. It is marked that the miniaturization process is easily done with the help of fractal geometry because of the self-similarity characteristics and a feature that fills space [7]-[8]. Fractal geometries resembling Koch snowflake [7][8][9], Minkowski [10]-[11] and Sierpinski triangles [4][7][12], are studied for UWB antenna design. For generation, multiband Koch fractal is used in [16] and in [17], the Koch fractal iteration is used for

T. Kumari, A. N. Ghazali and A. Senapati are with School of Electronics Engineering Kalinga Institute of Industrial Technology Bhubaneswar, India. Emails: tejaswita.kumari11@gmail.com, abu.ghazalifet@kiit.ac.in and anupamafet@kiit.ac.in

the generation of the WLAN frequency. Tapered tree-shaped fractals for wireless applications in [19]-[20] are used for UWB. In [22], fractal ring resonator is used and in [23], fractal geometry is used for compactness for UWB applications. There are different types of UWB antennas reported recently [24] that use a DGS technique for achieving super wide band, [25] uses a transparent antenna implanted on a solar-cell substrate and achieves super wideband. In [26], a stingray-shaped antenna is introduced and the CPW technique is used, where the peak gain of the antenna is 3.5 dBi. There are various antennas reported [27][28][29] that use DGS and CPW techniques to achieve the UWB bandwidth. [30] introduces a metasurface-based MIMO antenna, in this antenna, the isolation is enhanced by using the shorting pin and slot. The diversity gain is 9.99 dB.

It is observed that because of discontinuities and curves existing in the fractal antenna, the electromagnetic radiation is very proficient. Discontinuities and curves provide alteration in the current path, because of which the antenna properties improve, especially radiation [5].The conception that the Koch fractal geometry would yield a UWB outcome is based on these inherent properties of fractal structures, like multiband properties, miniaturization and space-filling, as well as enhanced bandwidth, improved radiation characteristics and frequency-independent properties researchers and antenna designers have explored various fractal geometries due to their unique characteristics, such as multiband operation, compact size and broadband capabilities, which align well with the requirements of UWB systems. This understanding, combined with simulations and empirical studies, likely led to the exploration and adoption of the Koch fractal structure for UWB-antenna applications.

The Koch fractal is very popular among researchers, but it also has some limitations, such as the Koch fractal structure's intricate geometry creating several challenges during the design and production stages. This is especially true when trying to achieve exact dimensions and iterations, especially when producing large quantities of the structure. Although fractal antennas have wideband capabilities, the Koch fractal has bandwidth limitations, making it difficult to attain wide frequency coverage without sacrificing other crucial antenna characteristics. Furthermore, matching the antenna's impedance to the system's impedance across its operating bandwidth is extremely difficult due to the complicated network of resonances and erratic patterns inherent in the Koch fractal structure. The more fractal iterations there are, the harder it is to shape the radiation pattern, which makes the directivity and radiation of the antenna less predictable. The proposed antenna has used the microstrip line for better performance. There are various ways to feed the antenna, one of which is CPW. CPW reduces the overall size of the antenna, but the reasons for choosing the microstrip feed line instead of CPW are various advantages of the microstrip line and the proposed design requirements, which can be stated as follows:

i. Microstrip lines are easier and cheaper to fabricate using standard printed circuit board (PCB) manufacturing processes. This simplicity in fabrication makes them more cost-effective and practical for mass production.

ii. Microstrip lines are easily integrated into standard PCB technologies, making them highly suitable for miniaturized and integrated designs.

iii. In some cases, microstrip lines can exhibit lower dispersion compared to CPW. This characteristic is beneficial in maintaining signal integrity at higher frequencies. Microstrip lines allow for simpler integration of other passive and active components on the same substrate, facilitating a more compact and integrated antenna system.

Following a comprehensive literature review, some limitations were identified, which can be summarized as follows:

i. Compliance with FCC regulations is a primary concern for ultra-wideband (UWB) technology. The UWB frequency range, typically spanning from 3.1 to 10.6 GHz in the United States, poses a considerable challenge in antenna design due to the need for effective operation across this wide frequency spectrum while managing issues related to size and performance.

ii. The substantial bandwidth of UWB signals necessitates antennas that can efficiently cover this extensive frequency range while maintaining consistent impedance matching.

iii. To maximize both the range and quality of UWB signals, antennas must consistently maintain a high level of radiation efficiency and a high gain.

The contributions of this paper are outlined as follows:

i. Because of their self-similar structure, Koch fractal antennas may function across a range of frequencies, enabling multiband operation without requiring significant changes to the antenna's design. This antenna exhibits resonance at three distinct frequencies; namely, 3.3 GHz, 6 GHz and 8.6 GHz.

ii. As per FCC, the bandwidth of the UWB antenna should be from 3.1 GHz to 10.6 GHz. The proposed antenna bandwidth spans between 2 GHz and 12.1 GHz, which covers the UWB range.

iii. To optimize the range and quality of ultra-wideband (UWB) signals, antennas need to consistently uphold a superior level of radiation efficiency and a high gain. With the proposed antenna boasting a peak gain of 8.94 dBi and an efficiency of 96.8%, these attributes significantly bolster its position as a formidable candidate for the UWB frequency band.

iv. The achieved three distinct resonance frequencies; namely, 3.3 GHz, 6 GHz and 8.6 GHz, are used in many different technological fields, including sensing, communication, radar systems and industrial applications and they take advantage of the special qualities that these frequency bands have to offer. Starting with the 3.3 GHz, within the microwave frequencies, these antennas power high-speed data transfers in 5G networks, enabling applications, like HD video streaming and swift mobile communication. The 6 GHz band, a cornerstone of Wi-Fi 6E, fuels seamless, high-speed connections in dense areas, such as stadiums and urban zones. Meanwhile, the 8.6 GHz frequency, part of the millimeter-wave spectrum, drives specialized high-speed, short-range communications, like WPAN and WBAN, as well as industrial, scientific and research applications. Together, these frequencies in ultraband antennas cater to a wide range of communication needs, balancing data rates, range and specific application requirements, thereby helping with precision in control systems, asset tracking and short-range sensing.

This paper starts by presenting an "introduction" that discusses fractal design concepts and challenges, followed by Sections 2 and 3 finalizing the Koch fractal design approach for fabrication. Patch-antenna design is carried out by a parametric study of the proposed UWB antenna. In Section 4, result analysis is conducted, followed in Section 5 by time domain analysis. Comparison with other reviewed references is shown in Section 6. This is followed by a "Conclusion", post-analysis of results and outcomes and suggestions for future work.

2. ANTENNA DESIGN APPROACH AND THEORY

The UWB antenna under consideration is constructed by implementing Koch fractal geometry along the edges of an octagonal shape. This antenna design represents a fusion of fractal geometries and conventional antenna technology. In fractal geometry, various segments are in different scales that come up again and again. Dimension and length [13] are derived using the following formulae:

$$D = \frac{\log(N)}{\log(r)} \tag{1}$$

$$l = h\left(\frac{N}{r}\right)^{n} \tag{2}$$

where, N= number of segments of geometry, h =length of curve, n = iteration number, r = number of segments divided by each iteration.

The algorithm of the iterative function system (IFS) is used to create the Koch fractal geometries. IFS is a very effective and useful method for generating any kind of fractal geometries. Translation, scaling and rotation are a few of the transformations used by IFS [10]. These changes are expressed as follows:

$$W\begin{bmatrix} x \\ y \end{bmatrix} = \begin{bmatrix} \frac{1}{r}cos\theta & \frac{-1}{s}sin\theta \\ \frac{1}{r}sin\theta & \frac{1}{s}cos\theta \end{bmatrix}\begin{bmatrix} x \\ y \end{bmatrix} + \begin{bmatrix} e \\ f \end{bmatrix} \tag{3}$$

where, scaling factor = r and s along the x and y axes, rotation angle=θ in the x-y plane and linear translations = e and f in the x axis and y axis, respectively.

Koch curve linear transformation matrices using IFS [14] are defined as follows:

"Koch Fractal Octagonal Antenna with a Compact Design and Defected Ground Structure (DGS) for Ultra-Wideband (UWB) Wireless Usage," T. Kumari, A. N. Ghazali and A. Senapati.

$$W0 = \begin{bmatrix} \frac{1}{3} & 0 & 0 \\ 0 & \frac{1}{3} & 0 \\ 0 & 0 & 0 \end{bmatrix} \tag{4}$$

$$W1 = \begin{bmatrix} \frac{1}{3}cos45° & -\frac{1}{3}sin45° & \frac{1}{3} \\ \frac{1}{3}sin45° & \frac{1}{3}cos45° & 0 \\ 0 & 0 & 1 \end{bmatrix} \tag{5}$$

$$W2 = \begin{bmatrix} \frac{1}{3}cos45° & \frac{1}{3}sin45° & \frac{1}{2} \\ \frac{1}{3}sin45° & \frac{1}{3}cos45° & \frac{1}{2}cos45° \\ 0 & 0 & 1 \end{bmatrix} \tag{6}$$

$$W3 = \begin{bmatrix} \frac{1}{3} & 0 & \frac{2}{3} \\ 0 & \frac{1}{3} & 0 \\ 0 & 0 & 1 \end{bmatrix} \tag{7}$$

$$F = \begin{bmatrix} 0 & 0 \\ 0 & 0 \\ 1 & 1 \end{bmatrix} \tag{8}$$

$$[xy_0 = W_0F, xy_1 = W_1F, xy_2 = W_2F, xy_3 = W_3F]$$

$$P = [xy_0 \quad xy_1 \quad xy_2 \quad xy_3] \tag{9}$$

where P is the all-coordinate point, which is generally used for fractal geometry in each segment. The first iteration of the Koch fractal divides the initial length into three equal segments and then, two equal segments are substituted for the middle segment, as depicted in Figure 1. The Koch fractal curve is generated by the repetition of each iteration on each and every segment.

Further, this Koch fractal is introduced in the substrate at the edge of the octagonal structure. Figure 2. depicts the center Koch fractal which is the subtraction at the center of the octagonal structure of the antenna. Step-wise structure evaluation is depicted in Figure 3.

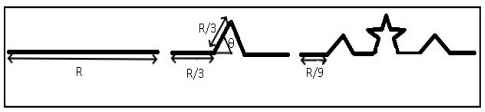

Figure 1. Generation of Koch fractal.

Figure 2. Centre Koch fractal.

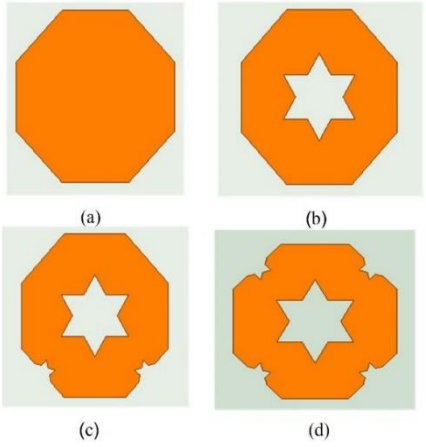

Figure 3. Koch fractal in octagonal geometry (a) Octagonal initiator, (b) First iteration, (c) Second iteration and (d) Third iteration.

Jordanian Journal of Computers and Information Technology (JJCIT), Vol. 10, No. 01, March 2024.

3. INVESTIGATION OF PROPOSED ANTENNA ACROSS DIFFERENT PARAMETERS

In this antenna design, the octagonal structure serves as the initiator, while the generator employs the principles of the Koch fractal. The primary objectives include achieving compactness, miniaturization, wide bandwidth and a direction-independent design. The octagonal structure gives two advantages (a) in terms of area and circumferences, octagonal shape is close to a circular structure and (b) it's easy to apply fractals on the edge of the octagonal shape. This combination encourages the geometry's bigger circumference in miniature dimension in contrast to alternative geometries, such as hexagonal, elliptical, circular geometries and so forth. Each segment is in charge of providing a resonant frequency; so, when they come together, wideband behavior becomes apparent in design [15]. Also, the octagonal shape provides a uniform radiation pattern across a wide frequency range and provides compactness to reduce interference. In Figure 7(c), the comparison S parameter between the different diameters is shown. For designing the proposed antenna, θ is the beginning structure's embarking on length R, where convergence of fractal geometry is provided by θ. In this proposed antenna, θ=450, R=1.6 mm for the edge of the octagonal iterative subtraction process and the center Koch S2 = 5 mm for the iterative subtraction process. It is evident that iteration of the Koch fractal in the octagonal generates the wide band and multiple resonant frequencies. Figure 4(a) depicts the progressive development stages of the proposed Koch fractal octagonal UWB antenna. Figure 4(b) shows the top view of the proposed antenna with measurement. Figure 4(c) depicts the bottom view of the proposed antenna with measurement. Figure 4(d) depicts the antenna with the microstrip feed line. Figure 4(e) shows the antenna with tapered feed.

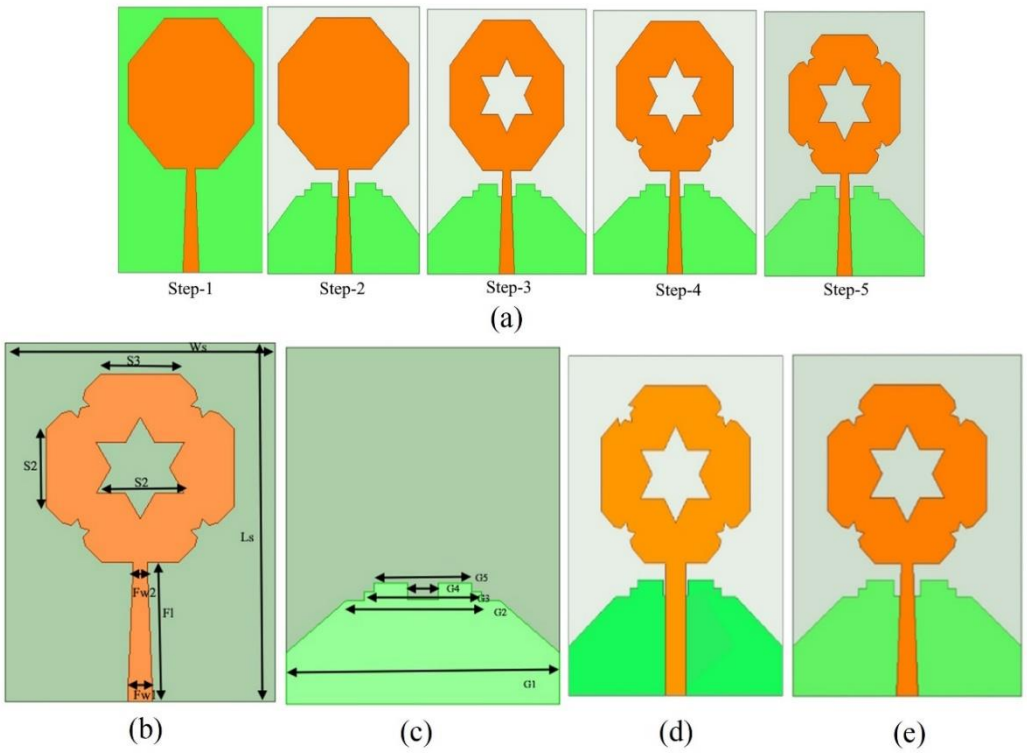

Figure 4(a) Progressive development stages of the proposed Koch fractal octagonal UWB antenna. Figure 4(b) Top view of the proposed antenna with measurement. Figure 4(c) Bottom view of the proposed antenna with measurement. Figure 4(d) Antenna with the micro-strip feed line. Figure 4(e) Antenna with tapered feed.

The proposed antenna uses a defected ground and the main purpose of using DGS is its unique features. The antenna's resonance frequency may be impacted by DGS configurations. Multiband or broadband capability can be achieved by introducing certain patterns or structures that alter the operating frequency or create various resonance frequencies, which can assist in reducing losses, enhancing antenna performance and decreasing surface wave propagation on the ground plane's structures, improving the isolation between antennas and the overall performance of an antenna array by reducing mutual coupling

between elements when utilized in arrays. Closely-spaced antenna structures can improve the isolation between antennas and the overall performance of an array by reducing mutual coupling between elements [24]. The proposed antenna used a step-wise structure which helps in improving isolation and the overall performance. Figure 4(a) Step-1 is an antenna with no DGS and Step-2, Step-3 and Step-4 have come with DGS. The effect of DGS is shown in Figure 8(a).

The antenna design presented in this study is fine-tuned through optimization and its features are examined using HFSS software, version 21. Antenna design and analysis are carried out on FR4 substrate. Rectangular substrate works best for the basic UWB antenna, where the reason behind choosing the rectangular substrate is that it provides a wide band and good radiation property [16]. εr =4.4 is the dielectric constant of the substrate and δ=0.02 is the loss tangent of the substrate. The parameters of the optimized Koch fractal octagonal antenna are displayed in Table 1.

Table 1. Parameters of optimized Kotch fractal octagonal UWB antenna.

Parameter	Dimension (mm)	Parameter	Dimension (mm)
L_S	34.3	Fw2	1.3
W_S	26.5	G1	26.5
S_2	5	G2	14.8
S_3	7.6	G3	10.4
h	1.6	G4	3.06
F_1	13.7	G5	9.4
FW_1	2.5	-	-

With the help of the basic formula of antenna-patch design [2], the overall length and breadth of the patch are calculated.

Effective Dielectric Constant:

$$\varepsilon_{reff} = \frac{\varepsilon_r+1}{2} + \frac{\varepsilon_r-1}{2}\left[1 + 12\frac{h}{w}\right]^{\frac{-1}{2}} \tag{10}$$

Width of patch:

$$W = \frac{1}{2f_r\sqrt{\mu_0\varepsilon_0}}\sqrt{\frac{2}{\varepsilon_r+1}} = \frac{v_0}{2f_r}\sqrt{\frac{2}{\varepsilon_r+1}} \tag{11}$$

Effective length of patch:

$$\frac{\Delta L}{h} = 0.412\frac{(\varepsilon_{reff}+0.3)(\frac{W}{h}+0.264)}{(\varepsilon_{reff}-0.258)(\frac{W}{h}+0.8)} \tag{12}$$

$$L_{eff} = L + 2\Delta L \tag{13}$$

Resonance frequency of Antenna:

$$(f_r)_{010} = \frac{1}{2L\sqrt{\varepsilon_r}\sqrt{\mu_0\varepsilon_0}} = \frac{v_0}{2L\sqrt{\varepsilon_r}} \tag{14}$$

The manufactured prototypes of the UWB antenna with a Koch fractal octagonal shape are produced and their attributes are verified within an anechoic chamber employing a Vector Network Analyzer (VNA). Figure 5 displays both the top and bottom views of the fabricated Koch fractal octagonal UWB antenna.

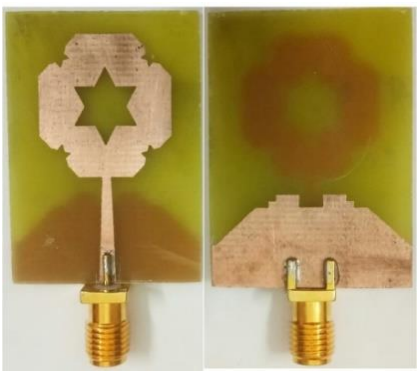

Figure 5. Top and bottom view of fabricated Koch fractal octagonal UWB antenna.

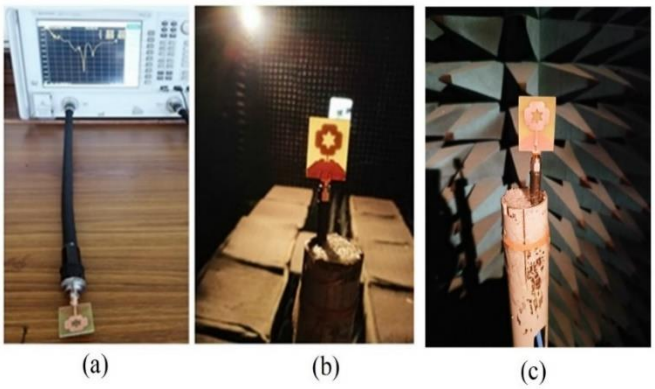

Figure 6. (a) Antenna under testing, (b) and (c) Antenna in anechoic chamber.

Following the fabrication process, the antenna design is subjected to laboratory testing, as illustrated in Figure 6. (a) Antenna under testing, (b) and (c) Antenna in anechoic chamber.

A parametric study of the antenna under consideration is conducted, which provides detailed information as well as the characteristics of the antenna. In ultrawide band antennas, geometrical and electrical parameters are affected by the desired characteristics. The main parameters of UWB antennas are dielectric constant of the used material (substrate), patch dimensions, feed gap, iteration geometric variation and dimensions of ground plane.

Figure 8 provides a sequential breakdown of the assessment of the proposed antenna. Step 1 illustrates the initial octagonal shape, Step 2 reveals the star Koch fractal subtraction in the center of the octagonal patch, Step 3 showcases the first two iterations on the lower side of the antenna and Step 4 displays the subsequent two iterations on the upper side of the recommended antenna. The ground plane for the proposed antenna is structured in a stepped shape, with its dimensions specified in Table 1.

The feed of the antenna used in the proposed design is in a tapered shape, which provides good impedance matching. From the literature survey, it is evident that for effective power transfer in the transmission line, which transmits the signal from the transmitter and the antenna itself, impedance matching is essential in antenna design. There are various ways that a tapered feed or tapered transmission line might help with impedance matching in antennas. The impedance of the transmission line and the antenna might gradually change in response to a tapering feed. The flow of power between the two is enhanced and reflections are decreased by this slow transition. By guaranteeing a smooth impedance transition, a tapered feed helps minimize standing waves by lowering reflections and increasing the amount of power that the antenna radiates. It facilitates improved impedance matching across a greater frequency range, which improves the antenna's performance. Figure 4(d) shows the antenna with a micro-strip feed line, while Figure 4(e) depicts the proposed antenna with tapered feed and the S parameter comparison graph is shown in Figure 7(b).

4. RESULTS AND ANALYSIS

All the results are analyzed in the lab and it is observed that all the results are up to the mark for the UWB antenna, as elaborated in the following sub-sections.

4.1 S Parameter

Figure 7(a) shows the stepwise S parameter of Koch fractal octagonal UWB antenna. Figure 7(b) compares S parameter between microstrip feed line and tapered feed line. Figure 7(c) Compares S parameter between different diameters of the radiator. Figure 7(d) compares S parameter between different heights of the substrate and shows the stepwise S parameter of the novel UWB Koch fractal antenna. From Figure 7(a), we can see in Step-1 the antenna having full ground not using DGS technology; the antenna does not get the desired bandwidth. In Step-2, the octagonal patch with DGS gets one resonant frequency at 3GHz and the bandwidth is narrow. After that, in Step-3, star Koch subtraction in the center of the octagonal patch improves the bandwidth of the antenna and resonates at 3.7 GHz. In Step-4, the first two iterations at the lower side of the proposed antenna provide the wide bandwidth and two resonant frequencies; 3.2GHz and 8.6 GHz. In Step-5, the second two iterations at the upper side of the proposed antenna increase bandwidth

"Koch Fractal Octagonal Antenna with a Compact Design and Defected Ground Structure (DGS) for Ultra-Wideband (UWB) Wireless Usage," T. Kumari, A. N. Ghazali and A. Senapati.

covering from 2 GHz to 12.1 GHz. This antenna is efficient at resonating at the triple frequencies of 3.3 GHz, 6 GHz and 8.6 GHz. Figure 7(b) shows S-parameter graph between microstrip feed line and tapered feed line. From the graph, it is evident that with the microstrip feed line, the proposed antenna is not getting the UWB bandwidth, but with the tapered feed the proposed antenna gets the desired UWB bandwidth 2 GHz -12.1 GHz with three resonant frequencies. Figure 7(c) shows the comparison graph of the different diameters of the patch. From the graph, it is evident that the optimized diameter is helpful for the proposed antenna for gating the UWB bandwidth. Figure 7(e) shows the S-parameter comparison graph for different heights of the substrate, where it is observed that the 1.6 height is helpful for the proposed antenna.

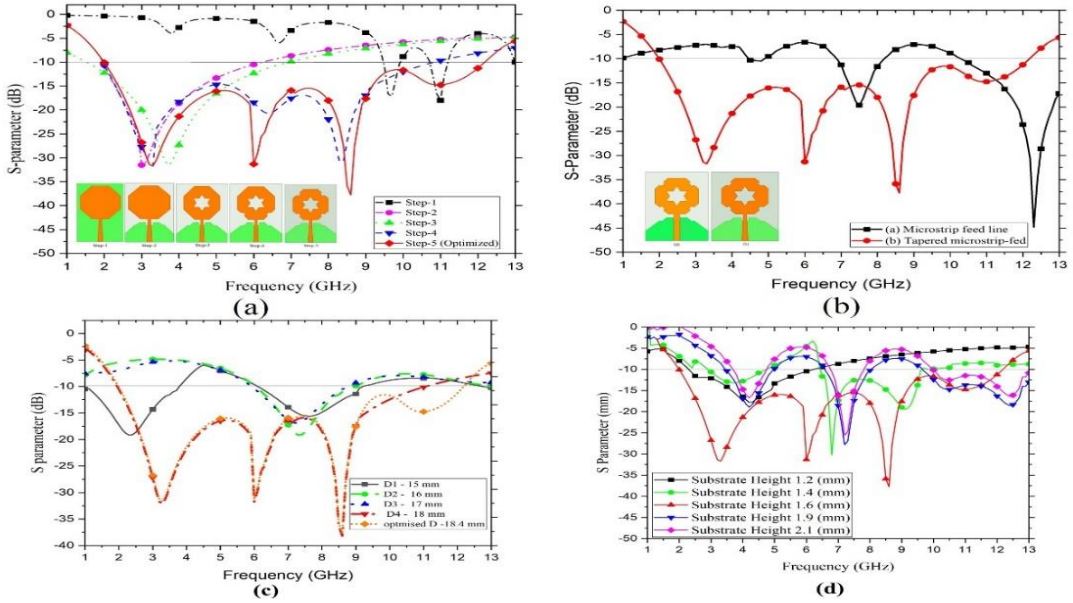

Figure 7. (a) The stepwise S parameter of Koch fractal octagonal UWB antenna, (b) S-parameter comparison between microstrip feed line and tapered feed line, (c) S-parameter comparison between different diameters of the radiator, (d) S-parameter comparison between different heights of the substrate.

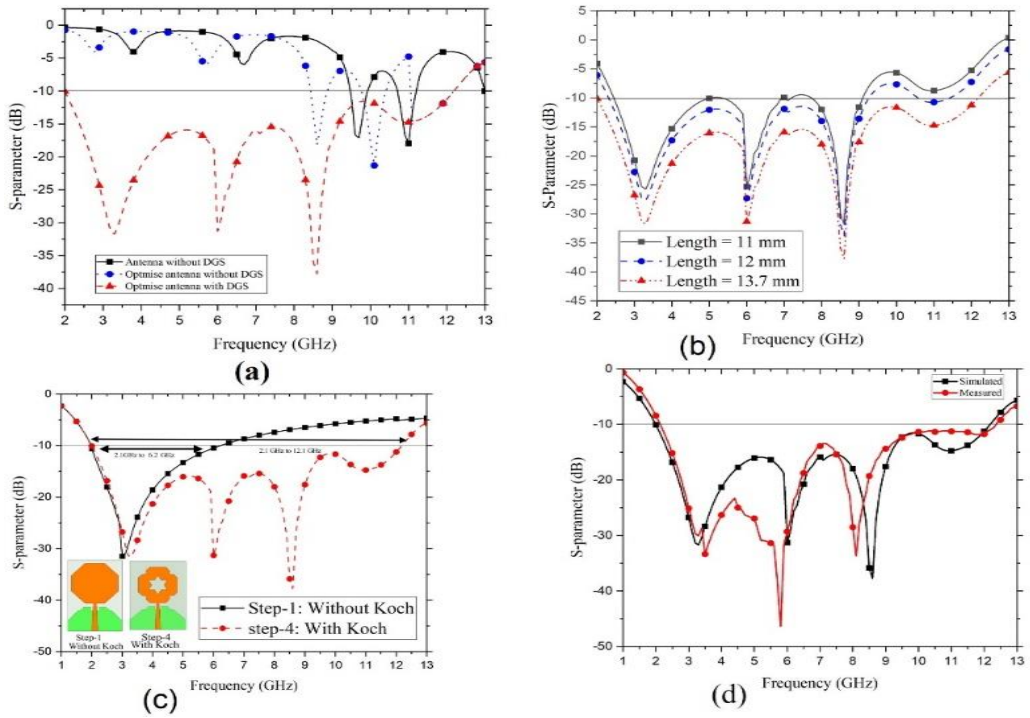

Figure 8. (a) S-parameter comparison with and without DGS, (b) S-parameter comparison of different feed lengths, (c) S-parameter comparison without Koch fractal and with Koch fractal octagonal UWB antenna, (d) Simulated and measured S parameters of the proposed antenna.

Figure 8 represents the parametrical study of the proposed antenna. Figure 8(a) shows the comparison graph of the proposed antenna, where in the base of the ground from the graph it is clear that the Step-1 antenna without DGS does not get the desired bandwidth. The optimized antenna without DGS also does not get the desired properties of UWB. Step-4 antenna optimized the proposed properties with DGS help for the desired bandwidth. Figure 8(b) shows the comparison graph of the different feed lengths of the proposed antenna and Figure 8(c) shows the comparison graph effect of the Koch fractal (with and without) in the proposed antenna, while Figure 8(d) depicts simulated and measured S parameters of the proposed antenna.

Here, we observe that the S parameter of the proposed antenna is below -10 dB and the triple resonance frequencies obtained are 3.3 GHz, 6 GHz and 8.6 GHz. It is observed that because of losses created by the SMA connector, the measurement surrounding and the fabrication tolerance, some discrepancies are shown in the results.

4.2 Radiation Pattern

Simulated and measured E-plane and H-plane radiation patterns at the resonant frequencies 2 GHz and 3.3 GHz of Koch fractal octagonal UWB antenna are shown in Figure 9. We observe that the radiation pattern at both frequencies is omnidirectional. Figure 10 shows the simulated and measured E-plane and H-plane radiation patterns at the resonant frequencies of 6 GHz and 8.6 GHz. Figure 11 shows the simulated and measured (a) E-plane and (b) H-plane radiation patterns at the resonant frequency of 12 GHz. Here, the three main resonant frequencies the beginning 2 GHz, the center 6 GHz and the end 12.1 GHz as well as the frequencies 3.3 GHz and 8.6 GHz are taken for the observation of the radiation pattern and Figure 11(c) shows the impedance matching on the Smith chart of the proposed antenna. Achieving perfect impedance matching across the entire UWB spectrum might be challenging due to the wide frequency range. From the graph, it is evident that the impedance matching of the proposed antenna is acceptable.

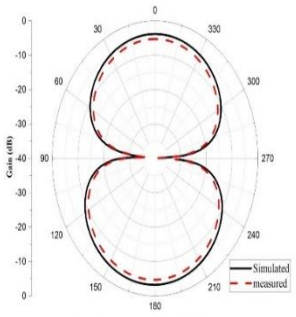

E Plane at 2.2 GHz

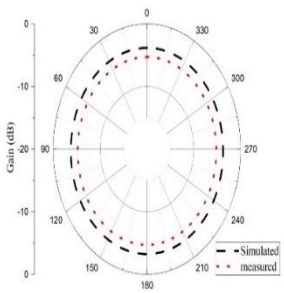

H plane at 2.2 GHz

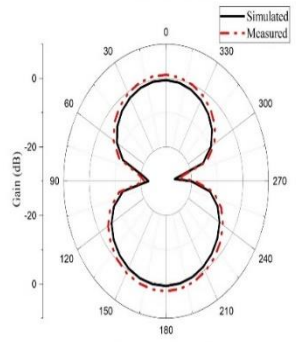

E plane at 3.3 GHz

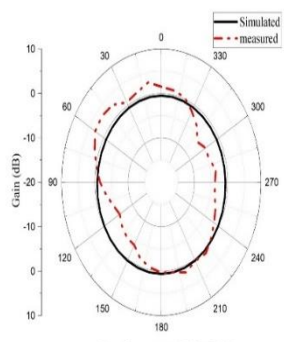

H plane at 3.3 GHz

Figure 9. Simulated and measured radiation pattern in the E plane and H plane at 2.2 GHz and in the E plane and H plane at 3.3 GHz of the proposed antenna.

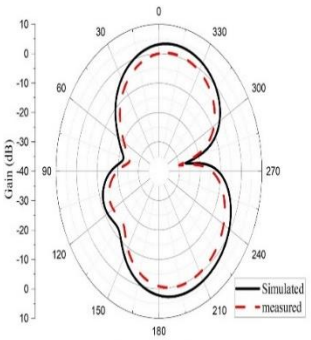

E plane at 6 GHz

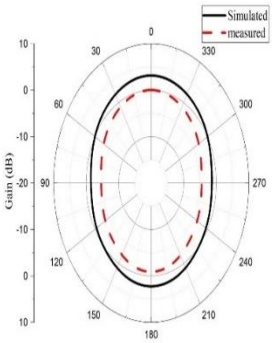

H plane at 6 GHz

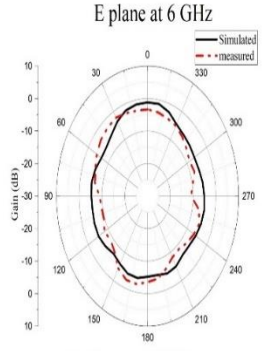

E plane at 8.6 GHz

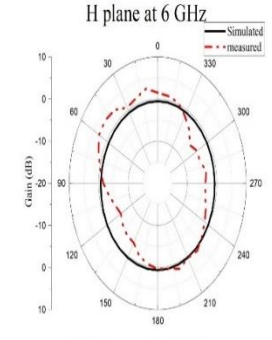

H plane at 8.6 GHz

Figure 10. Simulated and measured radiation pattern in the E plane and H plane at 6 GHz and in the E plane and H plane at 8.6 GHz of the proposed antenna.

We observe that the antenna is efficient in resonating at frequencies of 2 GHz, 3.3 GHz, 6 GHz and 8.6 GHz. In the case of E-plane and H-plane radiation patterns, it is evident that in both planes, the radiation pattern is omnidirectional.

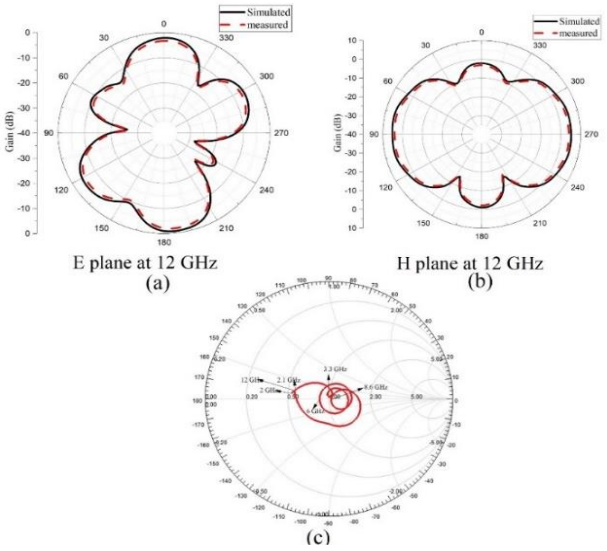

Figure 11. Simulated and measured radiation patterns (a) E-plane radiation patterns and (b) H-plane radiation patterns at 12 GHz of the proposed antenna and (c) Impedance matching on smith chart graph of the proposed antenna.

4.3 Radiation Efficiency

Radiation efficiency is also analyzed in this paper. Figure 12 shows the simulation followed by measured radiation efficiency *vs.* frequency graph. It is observed that during the resonant frequencies of 3.3 GHz, 6 GHz and 8.6 GHz, the radiation efficiency is between 92 and 96%. It is also evident that simulated radiation efficiency and measured radiation efficiency are flat around 2 GHz - 5.5 GHz.

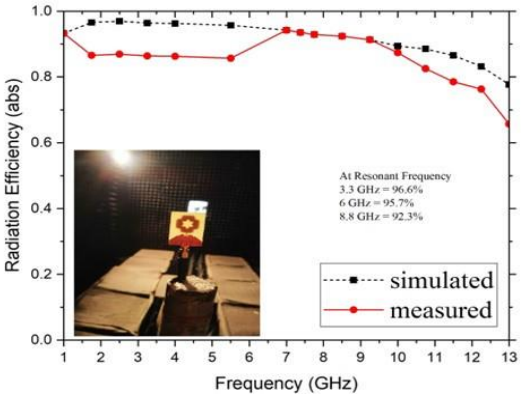

Figure 12. Radiation efficiency for the proposed Koch fractal octagonal UWB antenna.

4.4 Surface Current Distribution

Figure 13 and Figure 14 depict the Koch fractal antenna's sufface-current distribution at resonance

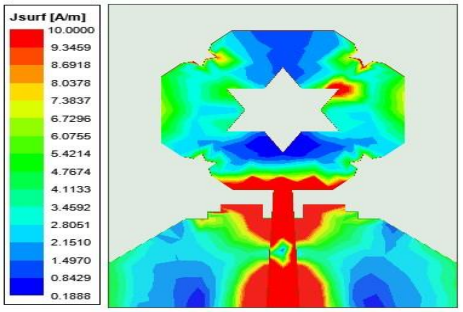

Figure 13. Surface-current distribution at resonant frequency of 3.3 GHz of the proposed Koch fractal octagonal UWB antenna.

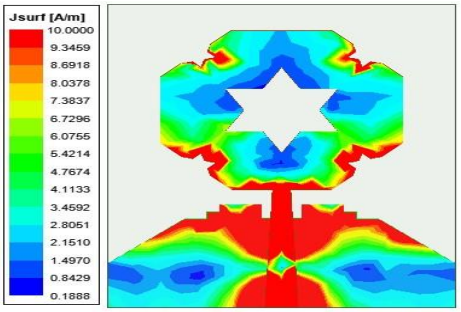

Figure 14. Surface-current distribution at resonant frequency of 8.6 GHz of the proposed Koch fractal octagonal UWB antenna.

frequencies of 3.3 GHz and 8.6 GHz. It is observed that at 3.3 GHz, the current is concentrated near the feed, but at 8.6 GHz, the surface current gathers surrounding the feed and the first half of the Koch antenna, which shows the accomplishment of the optimum impedance matching.

4.5 Gain

Figure 15 depicts simulated and measured gain of the Koch fractal octagonal antenna. Here, it was observed that the maximal gain of the designed antenna is 6.79 dB at 12.25 GHz. The overall gain is up to the mark for the UWB antenna.

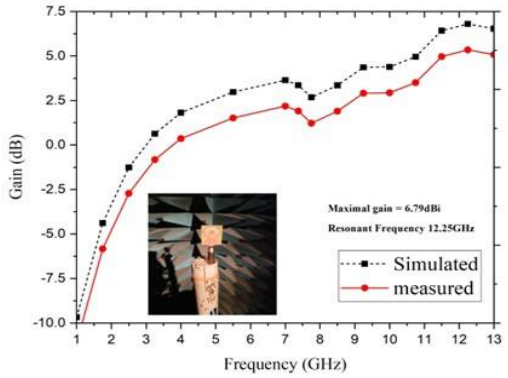

Figure 15. Peek gain *vs.* frequency graph of proposed Koch fractal octagonal UWB antenna.

5. TIME DOMAIN ANALYSIS

In the frequency domain, the antenna system demonstrates distinct properties, such as gain, polarization and directivity. Yet, examining the time domain provides the precise performance requirements for ultra-wideband antennas. This study sets important standards for impulse-oriented systems and confirms that they meet the requirements of the intended application. Time-domain characteristics, such as group delay, input and output correlation coefficients and fidelity-factor analysis, are explained in this section.

The correlation coefficient signifies the maximum correlation between two signals at a time delay τ, indicating the resemblance between the transmitted and received pulses. A maximum correlation coefficient of 0.9 denotes an almost complete similarity between the received and input signals of the proposed antenna [25]. The mathematical expression for the time correlation coefficient is calculated with the help of Equation 15.

$$F = max \frac{\int_{-\infty}^{+\infty} s_{t_x}(t) s_{t_x}(t-\tau) dt}{\sqrt{\int_{-\infty}^{+\infty} |s_{t_x}(t)|^2 dt \int_{-\infty}^{+\infty} |s_{r_x}(t)|^2 dt}} \quad (15)$$

where, S_{tx} = transmitter, S_{rx} = receiver and τ = time delay.

Antennas with a greater fidelity factor provide transmitted signals with less distortion and better precision. This is closely related to having a larger bandwidth, which makes it possible to send and receive a wider range of frequencies efficiently. High-fidelity factor antennas are essential for maintaining clear and dependable signal transmission in applications like microwave imaging, where accuracy and precision are critical. This eventually improves the imaging-process quality and resolution [26]. The transmitted (T_X) and received (R_X) pulses, designated as T^n and R^n, respectively, are normalized using Equations 16 and 17. To compare the pulses' waveforms or shapes rather than their absolute amplitudes, this normalization step is necessary. To emphasize the shapes or patterns of the pulses rather than their magnitudes, the pulses are normalized, particularly when the R_X pulses' amplitude is smaller than the T_X pulses' magnitude. Equation 18 is used to find the fidelity factor. In the face-to-face configuration, the proposed antenna has a higher fidelity factor of 90.2; so, it is evident that the proposed antenna has less distortion and better precision.

$$T_s^n = \frac{T_S(t)}{\sqrt{\int_{-\infty}^{+\infty} |T_S(t)|^2 dt}} \quad (16)$$

$$R_s^n = \frac{R_S(t)}{\sqrt{\int_{-\infty}^{+\infty} |R_S(t)|^2 dt}} \quad (17)$$

$$FF = max \int_{-\infty}^{+\infty} T_s^n(t) R_s^n(t)(t+\tau)dt \quad (18)$$

Another crucial performance metric for ultra wideband antennas is the group delay, which signifies the alteration in the phase of the transmitted signal concerning the frequency. In ultra-wideband (UWB) antennas, group delay signifies the time that it takes for diverse frequency parts within the transmitted signal to traverse the antenna or system. It's vital for UWB antennas spanning broad frequencies, revealing how these frequency elements experience delays within the antenna setup. Consistent group delay is crucial in UWB applications, as it upholds the timing relationships among frequencies, ensuring that these signal components reach their destinations without distortion or phase issues and maintaining signal accuracy and integrity.

In ultra-wideband (UWB) antennas, the group delay can be mathematically represented by deriving the phase response concerning frequency. If the phase response ϕ(ω) of the antenna system is known as a function of angular frequency ω, the group delay τ can be computed by taking the negative derivative of the phase concerning angular frequency. Group delay is calculated with the help of Equation 19.

$$\tau = \frac{\delta\theta(\omega)}{\delta\omega} \quad (19)$$

Here, τ=group delay, $\phi(\omega)$ =phase response of the antenna system and ω = angular frequency.

To compute the correlation coefficient, we utilize a wideband Gaussian pulse as the input signal transmitted through the antenna, as demonstrated in Figure 16 The transmitter and receiver antennas are positioned 17 cm apart at various angles ϕ (0°, 45°, 90°) in the XZ plane. To find out the separating distance of the transmitter and receiver antennas, Equation 20 is used.

$$FarField \geq \frac{2D^2}{\lambda} \quad (20)$$

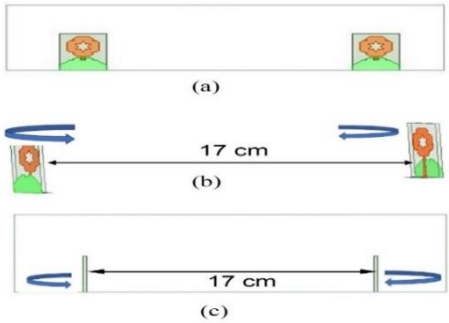

Figure 16. The transmitter antenna and receiver antenna are positioned 17 cm apart on the XZ plane (a-c), at various angles ϕ (0°, 45°, 90°).

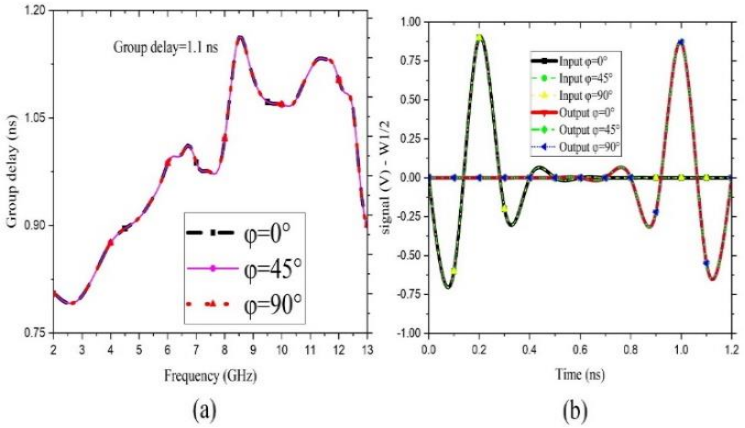

Figure 17. Time-domain characteristic graph (a) group-delay graph for ϕ(0°, 45°, 90°) on the XZ plane at various angles ϕ (0°, 45°, 90°) (b) graphs depicting the correlation coefficient.

Figure 17(a) shows the group-delay graph at various angles ϕ (0, 45, 90) degrees. In Figure 17(b), the graphs depicting the correlation coefficient are displayed for observation. The time-domain characteristics are acceptable for UWB. The group delay is 1.1 ns.

6. ANALYSIS IN RELATION WITH OTHER REVIEWED REFERENCES

The analysis of other reviewed references' antenna in terms of material used, dimension of antenna, operating band and gain are listed in Table 2. It has been noticed that the current work shows bandwidth enlargement. Moreover, the antenna size is smaller than in the works presented.

Table 2. Analysis of relations with other antennas.

Ref. No.	Material Used	Antenna Dimension mm^3	Operating Band (GHz)	Gain (dBi)
[9]	*FR*4	23.5x26.5x6	1.4-10.4	NR
[10]	RT/Duroid 5880	16.5x13.5x0.787	3.1-10.6	NR
[12]	Taconic	67x84x1	0.5-13.5	3.5-7
[13]	FR4	23.5x15x1.6	2.3-14	6.3
[16]	FR4	40x1.6x1.6	2-10	NR
[17]	FR4	30x30x1.6	2.3-13.2	5.5
[18]	FR4	60x55x1.59	NR	7.37
[19]	FR4	18.5x9.2x1.6	4.3-15.5	7.37
[20]	Taconic	30x40x0.8	3.3-11	5.74
[22]	FR4	40x24.5x1.6	NR	9.02
[23]	RT/Duroid 5880	24x30x0.787	3-12.7	6.1
[24]	Roger 5880	35 × 35 × 1.57	3.08-40.9	5.9
[25]	Plexi-glass	29× 27 × 1.6	2-32	10.6
[26]	RO5880 RF teflon	26× 29 × 0.787	3.8-12.7	3.5
[27]	RO5880	52× 26 × 0.787	2.3-11.5	8.4
[28]	FR4	14× 18 × 1.6	3.3-11.5	1.4
[29]	FR4	49.35x98.7x1.6	1-4.4	NR
[30]	RO4003C	71.6x71.6x3.118	3.27-3.82	8.1
[PW]	FR4	34.3 x 26.5 x 1.6	2-12.1	8.94

[*PW=proposed work,*NR = not reported].

Hence, it can be concluded that the suggested design of a single-element UWB antenna utilizing the Koch fractal octagonal structure is well-suited for UWB applications.

7. CONCLUSION

In this paper, a Koch fractal octagonal antenna is proposed for the ultra wideband (UWB) frequency-range applications. The uniqueness of this paper resides in its innovative use of the Koch fractal octagonal geometry to design an ultra wideband antenna that achieves miniaturization, compactness, wideband operation, high efficiency and multiple resonances. The combination of these features makes it a promising candidate for various wireless communication applications.

The paper introduces an innovative antenna design that utilizes a Koch fractal octagonal geometry. This choice of geometry is not commonly seen in traditional antenna designs, which makes it an innovative approach. The Koch-fractal use in the antenna design serves a dual purpose. It aids in miniaturization, meaning that the antenna can be made smaller while maintaining or enhancing its performance. Additionally, the fractal geometry contributes to the compactness of the antenna.

The proposed antenna's resonance at three specific frequencies (3.3 GHz, 6 GHz and 8.6 GHz) is another notable feature. This could potentially find applications in multi-frequency communication systems or frequency-selective applications. The antenna design presented provides a substantial bandwidth spanning from 2 GHz to 12.1 GHz. This kind of wide bandwidth is essential for UWB applications, This necessitates the capacity to send and receive signals across a wide spectrum of frequencies. The maximum gain of the antenna is 8.94 dBi at 12.25 GHz. The overall efficiency of the antenna is 96.8%. The time-domain characteristics are acceptable for UWB, where the group delay is

1.1 ns. The proposed antenna has a high fidelity factor of 90.2 and the correlation coefficient is 0.9, which makes the antenna a good candidate for UWB.

The paper introduces the significance of antenna design in modern wireless communication systems. It briefly mentions the challenges and the need for antennas with multiband operation, compact size, expanded bandwidth, high gain and high efficiency. These are the advantages of the proposed antenna:

Multiband Operation: The self-similar structure of the proposed Koch fractal antenna enables seamless operation across a wide range of frequencies. This unique design characteristic facilitates multiband functionality without necessitating significant alterations to the antenna's original design. The inherent scalability and self-similarity empower the antenna to operate efficiently across various frequency bands, marking a significant advancement in antenna versatility.

Compact Size: The fractal architecture of Koch-fractal antennas allows for remarkable miniaturization, rendering them ideal for integration into diminutive wireless devices, like RFID tags and smartphones. This inherent compactness without compromising performance positions these antennas as pivotal components for the next generation of portable communication technologies.

Expanded Bandwidth: Compared to conventional antennas, fractal antennas, including the proposed design, boast notably larger bandwidths. This expanded bandwidth offers unparalleled flexibility in signal transmission and reception, facilitating the accommodation of diverse data streams and improving overall communication reliability and performance.

High Gain and Efficiency: Maintaining consistently high efficiency throughout the ultra-wideband (UWB) spectrum, the proposed antenna stands out for its exceptional gain. The inherent design features optimize signal transmission and reception, resulting in amplified signal strength and reliability across the designated frequency range.

Summarizing the pivotal advantages presented by the proposed Koch fractal octagonal antenna, the proposed antenna has various applications. The bandwidth of 2 GHz to 12.1 GHz and the resonant frequencies of 3.3 GHz, 6 GHz and 8.6 GHz of the proposed antenna are important in the context of ultra-wideband (UWB). These various frequency allotments serve a variety of purposes according to regulatory requirements, bandwidth requirements, range constraints and interference considerations. Such antennas are used in many different technological fields, including sensing, communication, radar systems and industrial applications and they take advantage of the special qualities that these frequency bands have to offer. Starting with the 3.3 GHz, within the microwave frequencies, these antennas power high-speed data transfers in 5G networks, enabling applications, like HD video streaming and swift mobile communication. The 6 GHz band, a cornerstone of Wi-Fi 6E, fuels seamless, high-speed connections in dense areas, such as stadiums and urban zones. Meanwhile, the 8.6 GHz frequency, part of the millimeter-wave spectrum, drives specialized high-speed, short-range communications, like WPAN, WBAN, industrial, scientific and research applications. Together, these frequencies in ultra-band antennas cater to a wide range of communication needs, balancing data rates, range and specific application requirements, helping with precision in control systems, asset tracking and short-range sensing.

Future aspects of the proposed antenna are to improve the design for more applications in UWB, by designing the MIMO antenna, as well as the reconfigurable antenna.

REFERENCES

[1] Revision of Part 15 of the Commissions' Rule Regarding Ultra-wideband Transmission System, First Report and Order, "Federal Communications Commission FCC 02-48," Washington, Apr. 2002.

[2] C. A. Balanis, Antenna Theory Analysis and Design, 4th Edition, John Wiley & Sons, Inc., Hoboken, New Jersey, 2016.

[3] D. H. Werner, R. L. Haupt and P. L. Werner, "Fractal Antenna Engineering: The Theory and Design of Fractal Antenna Arrays," IEEE Antennas and Propagation Magazine, vol. 41, no. 5, pp. 37-59, 1999.

[4] J. Anguera, C. Puente, C. Borja and J. Soler, "Fractal-shaped Antennas: A Review," Encyclopedia of RF and Microwave Engineering, vol. 2, pp. 1620–1635, DOI: 10.1002/0471654507.eme128, 2005.

[5] C. Borja and J. Romeu, "On the Behaviour of Koch Island Fractal Boundary Micro-strip Patch Antenna," IEEE Transactions on Antennas and Propagation, vol. 51, no. 6, pp. 1281–1291, 2003.

[6] V. V. Reddy and N. V. S. N. Sarma, "Triband Circularly Polarized Koch Fractal Boundary Microstrip Antenna," IEEE Antennas and Wireless Propagation Letters, vol. 13, pp. 1057-1060, 2014.

[7] M. R. Haji-Hashemi, M. M. M. Sadeghi and V. M. Moghtadai, "Space-filling Patch Antennas with CPW Feed," Proc. of Progress in Electromagnetics Research Symposium, pp. 26–29, Cambridge, USA, 2006.

[8] M. G. Fekadu and S. N. Sinha, "UWB Fractal Slot Antenna Designs," Proc. of the 2011 IEEE Int. Conf. on Microwaves, Communications, Antennas and Electronics Systems (COMCAS), pp. 1–4, DOI: 10.1109/COMCAS.2011.6105799, 2011.

[9] S. Tripathi, A. Mohan and S. Yadav, "Ultra wideband (UWB) Antenna Using Minkowski Like Fractal Geometry," Microwave and Optical Technology Letters, vol. 56, no. 3, pp. 2273–2279, 2014.

[10] S. Tripathi, A. Mohan and S. Yadav, "A Multi Notched Octagonal Shaped Fractal UWB Antenna," Microwave and Optical Technology Letters, vol. 56, no. 11, pp. 2469–2473, 2014.

[11] C. Puente-Baliarda, J. Romeu, R. Pous and A. Cardama, "On the Behavior of the Sierpinski Multiband Fractal Antenna," IEEE Transactions on Antennas and Propagation, vol. 46, no. 4, pp. 517-524, DOI: 10.1109/8.664115, April 1998.

[12] D. Li and J.-f. Mao, "A Koch-like Sided Fractal Bow-tie Dipole Antenna," IEEE Transactions on Antennas and Propagation, vol. 60, no. 5, pp. 2242-2251, DOI: 10.1109/TAP.2012.2189719, May 2012.

[13] S. Tripathi, A. Mohan and S. Yadav, "A Compact UWB Koch Fractal Antenna for UWB Antenna Array Applications," Wireless Personal Communications, vol. 92, pp. 1423–1442, 2017.

[14] S. Dhar, R. Ghatak, B. Gupta and D. R. Poddar, "A Wideband Minkowski Fractal Dielectric Resonator Antenna," IEEE Transactions on Antennas and Propagation, vol. 61, no. 6, pp. 2895–2903, 2013.

[15] N. Tasouji, J. Nourinia, C. Ghobadi and F. Tofigh, "A Novel Printed UWB Slot Antenna with Reconfigurable Band-notch Characteristics," IEEE Antennas and Wireless Propagation Letters, vol. 12, pp. 922–925, 2013.

[16] A. Gobinath, N. Sureshkumar, K. K. Hema, T. Sureka and B. Pavithra, "Design of Koch Fractal Antenna for Wireless Applications," International Journal of Engineering Research & Technology (IJERT) NCIECC-2017, vol. 5, no. 9, 2017.

[17] S. Mythili, K. Akshaya, B. Charanya and K. Ayyappan, "Design and Analysis of Koch Fractal Antenna for WLAN Applications," ICTACT Journal on Microelectronics, vol. 06, no. 02, pp.923-927, 2020.

[18] M. Gupta and V. Mathur, "Koch Boundary on the Square Patch Microstrip Antenna for Ultra Wideband Applications," Alexandria Engineering Journal, vol. 57, no. 3, pp. 2113-2122, 2018.

[19] S. Singhal, T. Goel and A. Kumar Singh, "Inner Tapered Tree-shaped Fractal Antenna for UWB Applications," Microwave and Optical Technology Letters, vol. 57, no. 3, pp. 559-567, 2015.

[20] H. Z. Liu, J. C. Coetzee and K. Mouthaan, "UWB Antenna Array for Wireless Transmission along Corridors," Microwave and Optical Technology Letters, vol. 50, no. 4, pp. 886–890, 2008.

[21] S. Mahesh, A. Khairnar and M. Hasan, "A New Approach to Fractal Antenna Design for UWB Applications: An Analysis," Mathematical Statistician and Engineering Applications, vol. 71, no. 4, pp. 2326-9865, 2022.

[22] I. H. Nejdi et al., "UWB Circular Fractal Antenna with High Gain for Telecommunication Applications," Sensors, vol. 23, no. 8, p. 4172, 2023.

[23] M. A. Khan, U. Rafique, H. Ş. Savci, A. N. Nordin, S. H. Kiani and S. M. Abbas, "Ultra-wideband Pentagonal Fractal Antenna with Stable Radiation Characteristics for Microwave Imaging Applications," Electronics, vol. 11, no. 13, p. 2061, 2022.

[24] S. Ullah, C. Ruan, M. S. Sadiq, T. U. Haq, A. K. Fahad and W. He, "Super Wideband, Defected Ground Structure (DGS) and Stepped Meander Line Antenna for WLAN/ISM/WiMAX/UWB and other Wireless Communication Applications," Sensors, vol. 20, p. 1735, DOI: 10.3390/s20061735, 2020.

[25] M. Rohaninezhad et al., "Design and Fabrication of a Super-wideband Transparent Antenna Implanted on a Solar Cell Substrate," Scientific Reports, vol. 13, no. 1, p. 9977, 2023.

[26] H. Şerif Savcı, "A Four Element Stringray-shaped MIMO Antenna System for UWB Applications," Micromachines, vol. 14, no. 10, p. 1944, 2023.

[27] S. Hassan Kiani et al., "An Ultra-Wide Band MIMO Antenna System with Enhanced Isolation for Microwave Imaging Applications," Micromachines, vol. 14, no. 9, p. 1732, 2023.

[28] S. Hassan Kiani et al., "A Novel Shape Compact Antenna for Ultra Wideband Applications," Int. Journal of Antennas and Propagation, vol. 2021, p. 7004799, DOI: 10.1155/2021/7004799, 2021.

[29] A. Chowdhury and P. Ranjan, "A Novel Circularly Polarized, CPW-based MIMO Antenna for 5G-Wireless Communication in Sub-6 GHz Band," Int. Journal of Electronics Letters, DOI: 10.1080/21681724.2023.2266608, 2023.

[30] M. A. Sufian, N. Hussain, H. Askari, S. G. Park, K. S. Shin and N. Kim, "Isolation Enhancement of a Metasurface-based MIMO Antenna Using Slots and Shorting Pins," IEEE Access, vol. 9, pp. 73533-73543, 2021.

"Koch Fractal Octagonal Antenna with a Compact Design and Defected Ground Structure (DGS) for Ultra-Wideband (UWB) Wireless Usage," T. Kumari, A. N. Ghazali and A. Senapati.

ملخص البحث:

يقدّم هذ البحث هوائياً مُدْمَجاً ثماني الأضلاع مع بِنيةِ أساسٍ مشوَّهة مُصمَّماً للاستخدام في الاتّصالات اللاسلكية في نطاق التّردّدات فائقة العرض (UWB). ويؤدّي التصميم المقترح إلى الحصول على حجمٍ صغير لهوائي مُدْمَج ملائم للعمل في نطاق التّردّدات فائقة العرض. يَستخدِم الهوائي المقترح النّحاس كمادّةٍ موصلة على طبقةِ أساسٍ من نوع (FR-4) لها ثابت عزْلٍ كهربائي يساوي (4.4) و ظِلّ زاوية فقْد مقداره (0.02) و سُمْك يبلغ (1.6) ملم.

يحقّق الهوائي المقترح كسباً أقصى مقدارهُ (8.94) ديسيبل عند تردّدٍ مقداره (12.25) جيجاهيرتز، ويعمل في نطاقٍ تردّدي يمتدّ من (2) جيجاهيرتز إلى (12.1) جيجاهيرتز. وللهوائي المصمَّم في هذا البحث ثلاثة تردّدات رنين (3.3، و 6، و 8.6 جيجاهيرتز)، الأمر الّذي يمنحهُ فعاليةً عالية، حيث تبلغ فعاليته الكلية (96.8%) ، كما يبلغ معامل الارتباط له (0.9)، ممّا يجعله مرشَّحاً جيداً للاستخدام في نطاق التّردّدات فائقة العرض (UWB).

والجدير بالذّكر أنّ خصائص الهوائي المقتَرح تؤهّلهُ للاستخدام في شبكاتٍ لاسلكيةٍ متنوّعةٍ مثل (WPAN) و (WBAN)، كما يمتدّ استخدامه إلى التطبيقات الصّناعية؛ إذ يُساعد بدقّةٍ كبيرةٍ في أنظمة التّحكّم وتَتَبُّع الأصول والاستشعار قصيرالمدى وأنظمة الرّادار.

This article is an open access article distributed under the terms and conditions of the Creative Commons Attribution (CC BY) license (http://creativecommons.org/licenses/by/4.0/).